High Subglass Transitions Appearing in the Rigid Polyimides Derived from the Novel 1,6-Bis(4-aminophenyl)diamantane

Yaw-Terng Chern

Institute of Chemical Engineering, National Taiwan University of Science and Technology, Taipei, Taiwan 106, Republic of China

Received May 20, 1997; Revised Manuscript Received December 7, 1997

ABSTRACT: This work has synthesized new diamantane-based polyimides by reacting 1,6-bis(4-aminophenyl)diamantane (**5**) with various aromatic tetracarboxylic dianhydrides. Dynamic mechanical analysis (DMA) reveals that diamantane-based polyimides have three relaxations on the temperature scale between 0 and 500 °C. The low-temperature subglass relaxations, ranging from 150 to 200 °C, are typical β relaxations for standard polyimides. The relatively high-temperature β_1 subglass relaxations in polyimides **8** occur at a markedly higher temperature, i.e., approximately 300 °C, than typically observed in most other polyimides. The characteristic β_1 relaxation is associated with a step decrease in G′ and small transition peaks appearing in tan δ and G''. Moreover, the insensitivity of the β_1 subglass relaxation temperature to changes in the dianhydride demonstrates that the subglass process is localized largely within the diamine moiety. Their glass relaxations occur at extremely high temperatures exceeding 500 °C. These films had low dielectric constants ranging from 2.54 to 2.74, as well as low moisture absorptions less than 0.40%. In addition, the polyimides **8d** and **8e** are soluble in *o*-chlorophenol, chloroform, *N*-dimethylacetamide (DMAc), and tetrahydrofuran (THF). These films have tensile strengths to break values up to 124 MPa, elongation to break values up to 5.6%, and initial moduli up to 2.3 GPa. Interestingly, selective functionalization of 1,6-dibromodiamantane to 1,6- and 4,9-diphenyldiamantanes is attained using the catalysts $FeCl_3$ and $AlBr_3$, respectively.

Introduction

Thermally stable polymers have received extensive interest over the past decade due to increasing demands for high-temperature polymers as replacements for metals or ceramics in automotive, aerospace, and microelectronic industries. Polyimides are certainly one of the most successful class of high-temperature polymers and have found extensive application in the aviation, automotive, and electronic industries. However, they are frequently insoluble and unable to melt below their decomposition temperature. Therefore, processing in melt or solution is generally impossible. Many investigators have attempted to enhance their processabilities and solubilities by introducing either bulky groups or flexible chain into the polymer backbone or attaching bulky side groups.[1−7] In a similar manner, noncoplanar diamines and dianhydrides are quite effective in improving polyimides solubilities.[1,6,8]

Although diamantane has been investigated for many years, only a few examples of the polymers based on diamantane are known.[9−17] Previously, the 1,4-, 4,9-, and 1,6-diethynyldiamantanes were polymerized to yield clear thermoset resins that degraded between 518 and 525 °C in air or helium.[9] In that work colorless diamantane-based polybenzazoles were prepared via the established polyphosphoric acid polycondensation technique.[10] In addition, polycules based on diamantane have found specific applications in building dendritic materials.[11] Our recent work indicated that incorporating diamantyl groups into polyamides, polyesters, and poly(amide−imide)s allowed these polymers to have good thermal stabilities, high glass transition temperatures, and good retention of storage moduli above their glass transition temperatures.[12−16] Regarding the incorporation of diamantane into the polyimide, only one example of the polyimide has been reported by us.[17] However, polyimide films based on diamantane have not been successfully prepared.[17] Thus, the physical properties of a diamantane-based polyimide (except for thermal stability) have not been reported as well.

It has been reported that most aromatic polyimide films exhibited two relaxations at the temperatures exceeding 0 °C in their dynamic mechanical behaviors.[18−20] The subglass relaxation in most polyimides occurs between 50 and 200 °C. This relaxation in the well-studied polyimide pyromellic dianhydride−4,4′-oxydianiline has been attributed to interplane slippage.[18] Bernier et al. attributed the subglass relaxation in polyimides to rotation of phenyl groups.[19] Perena attributed this relaxation to oscillations of the phenyl groups in the diamine residue.[20] Investigation of the polyimides based on the rigid dianhydrides and diamines, these polyimides containing 2,2′-disubstituted benzidines have much higher subglass transitions, i.e., approximately 300 °C, than typically observed in most other polyimides.[21,22] In addition, an uncommon feature of these polyimides is a rather prominent subglass relaxation. Coburn et al. attributed this relaxation to main-chain rotational motion localized within the diamine (benzidine) segment.[21]

In this paper, we investigated the mechanical relaxation behaviors in rigid polyimides containing 1,6-bis(4-aminophenyl)diamantane in order to better understand the role of polyimide backbones on the occurrence of high subglass relaxation. Herein, we also successfully synthesize new polyimides involving 1,6-bis(4-aminophenyl)diamantane (**5**) by the polycondensation with aromatic tetracarboxylic dianhydrides **6**. The dielectric constants, moisture absorptions, coefficients of thermal expansion (CTE), solubilities, dynamic mechanical prop-

S0024-9297(97)00712-2 CCC: $15.00
Published on Web 02/24/1998

erties, and thermal properties of the polyimides are investigated as well. In addition, selective functionalization of 1,6-dibromodiamantane to 1,6- or 4,9-diphenyldiamantane is also investigated.

Experimental Section

Materials. Pyromellitic dianhydride (**6a**), 4,4′-carbonyldiphthalic anhydride (**6b**), 4,4-oxydiphthalic anhydride (**6c**), 4,4-hexafluoroisopropylidenediphthalic anhydride (**6d**), and 3,3′, 4,4′-biphenyltetracarboxylic dianhydride (**6f**) were purified by sublimation. *N*-Methyl-2-pyrrolidone (NMP) was purified by distillation under reduced pressure over calcium hydride and stored over 4 Å molecular sieves. Acccording to a previous method, 1,6-dibromodiamantane (**1**) was synthesized from norbornadiene in four steps.[12]

Herein, three steps were employed to synthesize bis[4-(3,4-dicarboxyphenoxy)phenyl] ether dianhydride (**6e**) by previous methods[5,23] from 4,4′-dihydroxydiphenyl ether. The corresponding bisphenol reacted with 4-nitrophthalodinitrile in anhydride−dimethyl sulfoxide in the presence of potassium carbonate as an acid acceptor to generate bis(ether dinitrile) which, subsequently, was then hydrolyzed to bis(ether diacid) and dehydrated to bis(ether anhydride).

Bis[4-(3,4-dicarboxyphenoxy)phenyl] Ether Dianhydride (6e): mp 238−240 °C; IR (KBr) 1849, 1772, 1612, 1475 cm^{-1}; MS (EI) *m/z* 494 (M^+, 100); ^1H NMR (400 MHz, DMSO-d_6) δ 7.09−7.20 (m, 12H, ArH), 7.76 (d, J = 8.28, Hz, 2H, ArH); ^{13}C NMR (100 MHz, DMSO-d_6) δ 116.07 (d, Ar), 118.25 (d, Ar), 120.32 (d, Ar), 121.83 (d, Ar), 125.51 (s, Ar), 131.43 (d, Ar), 136.59 (s, Ar), 150.38 (s, Ar), 153.56 (s, Ar), 159.71 (s, Ar), 167.39 (C═O), 168.50 (C═O). Crystal data: $C_{28}H_{14}O_9$, colorless crystal, 0.200 × 200 × 25 mm, triclinic $P\bar{1}$ with a = 8.0198(16) Å, b = 14.825(7) Å, c = 20.016(9) Å, α = 109.69(3)°, β = 91.79(3)°, γ = 94.66(3)°, and D_c = 1.473 g cm^{-3} for Z = 4, V = 2228.8(14) $Å^3$, T = 298 K, λ = 1.5418 Å, μ = 8.979 cm^{-1}, F(000) = 1020, and R_w = 0.091 for 3235 observed reflections, intensity variation <3%.

Synthesis of 1,6-Diphenyldiamantane (2). A 150 mL, three-necked, round-bottomed flask was charged with 1,6-dibromodiamantane (3.00 g, 8.68 mmol), 80 mL of benzene, and iron(III) chloride (0.500 g, 3.08 mmol). The mixture was heated to reflux for 12 h; the reaction was allowed to cool to room temperature. Next, the precipitate was filtered out, and the filtrate was washed with distilled water. The filtrate was then dried under reduced pressure. The crude product was crystallized from toluene to obtain **2** (1.35 g, 45.8%). The properties were as follows: mp 298−300 °C; IR (KBr) 3057, 2888, 2867, 1592, 1510 cm^{-1}; MS (EI) *m/z* 340 (M^+, 100); ^1H NMR (300 MHz, $CDCl_3$) δ 1.51−1.55 (m, 8H, H 3a, 5, 8a, 10a, 13, 14a), 1.74 (m, 2H, H 4, 9), 1.93−1.97 (d, J = 12.38 Hz, 4H, H 3e, 8e, 10e, 14e), 2.61 (m, 4H, H 2, 7, 11, 12), 7.17 (t, 2H, ArH), 7.31−7.42 (m, 8H, ArH); ^{13}C NMR (75 MHz, $CDCl_3$) δ 28.62 (C 4, 9), 33.96 (C 3, 8, 10, 14), 39.65 (C 2, 7, 11, 12), 42.39 (C 1, 6), 50.53 (C 5, 13), 125.64 (d, Ar), 126.09 (d, Ar), 129.02 (d, Ar), 149.64 (s, Ar). Anal. Calcd for $C_{26}H_{28}$: C, 91.76; H, 8.24. Found: C, 91.58; H, 8.18.

Synthesis of 4,9-Diphenyldiamantane (3) from 1,6-Dibromodiamantane. A 150 mL, three-necked, round-bottomed flask was charged with 1,6-dibromodiamantane (3.00 g, 8.68 mmol), 70 mL of benzene, and aluminum bromide (1.00 g, 3.75 mmol). The mixture was heated to reflux for 10 h, and the reaction was naturally cooled to room temperature. Next the precipitate was filtered out, and the filtrate was washed with distilled water. The filtrate was then dried under reduced pressure. The crude product was crystallized from toluene to obtain **3** (0.614 g, 20.8%): mp 278−280 °C; IR (KBr) 3013, 2888, 2867, 1597, 1491 cm^{-1}; MS (EI) *m/z* 340 (M^+, 100); ^1H NMR (300 MHz, $CDCl_3$) δ 1.97 (brs, 18H, hydrogen of diamantane), 7.18−7.21 (t, 2H, ArH), 7.30−7.42 (m, 8H, ArH); ^{13}C NMR (75 MHz, $CDCl_3$) δ 34.23 (C 4, 9), 37.51 (C 1, 2, 6, 7, 11, 12), 43.46 (C 3, 5, 8, 10, 13, 14), 125.08 (d, Ar), 125.59 (d, Ar), 128.13 (d, Ar), 150.50(s, Ar). Anal. Calcd for $C_{26}H_{28}$: C, 91.76; H, 8.24. Found: C, 91.65; H, 8.16. Crystal data: $C_{26}H_{28}$, colorless crystal, 0.150 × 400 × 40 mm, monoclinic P 21/n with a = 6.4218(20) Å, b = 19.619(4) Å, c = 7.9656(20) Å, β = 113.452(20)°, and D_c = 1.228 g cm^{-3} for Z = 2, V = 920.7(4) $Å^3$, T = 298 K, λ = 1.5418 Å, μ = 4.793 cm^{-1}, F(000) = 369, and intensity variation <3%.

Synthesis of 1,6-Bis(4-nitrophenyl)diamantane (4). 2 (2.00 g, 5.88 mmol) was suspended in 40 mL of glacial acetic acid, and 25 mL of fuming nitric acid was added dropwise. The resulting yellow solution was stirred for 5 days and then poured onto ice. The precipitated solid was collected by filtration yielding 2.03 g (80.3%) of **4**: mp >390 °C; IR (KBr) 2888, 2867, 1591, 1512, 1341, 751 cm^{-1}; MS (EI) *m/z* 430(M^+, 100), ^1H NMR (300 MHz, $CDCl_3$) δ 1.52−1.62 (m, 8H, H 3a, 5, 8a, 10a, 13, 14a), 1.83−1.87 (m, 6H, H 3e, 4, 8e, 9, 10e, 14e), 2.64 (brs, 4H, H 2, 7, 11, 12), 7.56 (d, J = 9.04 Hz, 4H, ArH), 8.21 (d, J = 8.98 Hz, 4H, ArH), ^{13}C NMR (75 MHz, $CDCl_3$) δ 27.45 (C 4,9), 33.11 (C 3,8,10,14), 38.81 (C 2,7,11,12), 42.51 (C 1,6), 49.02 (C 5,13), 123.87 (d, Ar), 126.37 (d, Ar), 145.65 (s, Ar), 156.53 (s, Ar). Anal. Calcd for $C_{26}H_{26}N_2O_4$: C,72.56; H, 6.05; N, 6.51. Found: C, 72.32; H, 5.97; N,6.45. Crystal data: $C_{26}H_{26}N_2O_4$, very pale yellow crystal, 0.100 × 150 × 20 mm, monclinic P 21/n with a = 11.1925(13) Å, b = 7.6790(21) Å, c = 11.8849(24) Å, β = 98.352(13)°, and D_c = 1.415 g cm^{-3} for Z = 2, V = 1010.6(4) $Å^3$, T = 298 K, λ = 0.7107 Å, μ = 0.895 cm^{-1}, F(000) = 456, and intensity variation <2%.

Synthesis of 1,6-Bis(4-aminophenyl)diamantane (5). A 150 mL, three-necked, round-bottomed flask was charged with **4** (1.00 g, 2.33 mmol), 10 mL of hydrazine monohydrate, 60 mL of ethanol and 0.02 g of 10 palladium on carbon (Pd−C). The mixture was heated to reflux for 16 h. The mixture was then filtered to remove the Pd−C, and the crude solid was recrystallized from *N*-dimethylacetamide (DMAc) to afford 0.764 g (88.6%) of white crystals: mp 372−374 °C; IR (KBr) 3431, 3356, 2890, 2867, 1622, 1515 cm^{-1}; MS(EI) *m/z* 370 (M^+, 100); ^1H NMR (400 MHz, $CDCl_3$) δ 1.44−1.54 (m, 8H, H 3a, 5, 8a, 10a,13, 14a), 1.69 (brs, 2H, H 4, 9), 1.95 (d, J = 12.48, 4H, H 3e, 8e, 10e, 14e), 2.49 (brs, 4H, H 2, 7, 11, 12), 3.54 (brs, 4H, NH_2), 6.67 (d, J = 8.42, 4H, ArH), 7.17 (d, J = 8.23 Hz, 4H, ArH); ^{13}C NMR (100 MHz, $CDCl_3$) δ 28.25 (C 4,9), 33.42 (C 3, 8, 10, 14), 39.34 (C 2, 7, 11, 12), 41.07 (C 1,6), 50.32 (C 5, 13), 115.50 (d, Ar), 126.48 (d, Ar), 139.62(s, Ar), 143.50 (s, Ar). Anal. Calcd for $C_{26}H_{30}N_2$: C, 84.32; H, 8.11; N, 5.05. Found: C, 84.13; H, 8.03; N, 4.98.

Characterization. A Bio-Rad FTS-40 FTIR spectrophotometer was used to record IR spectra (KBr pellets). In a typical experiment, an average of 20 scans per sample was made. MS spectra were obtained by using a JEOL JMS-D300 mass spectrometer. ^1H and ^{13}C NMR spectra were recorded on Bruker AM-300WB or AM-400 Fourier transform nuclear magnetic resonance spectrometers using tetramethylsilane (TMS) as the internal standard. A Perkin-Elmer 240C elemental analyzer was used for elemental analysis. The X-ray crystallographic data were collected on a CAD-4 diffractometer. The analyses were carried out on a DEC station 3500 computer using NRCC SDP software. The melting points were obtained by a standard capillary melting point apparatus. Inherent viscosities of all polymers were determined at 0.5 g/dL using an Ubbelohde viscometer. Gel permeation chromatography (GPC) on soluble polymers were performed on an Applied Biosystem at 70 with two PLgel 5 μm mixed-C columns in the NMP/LiBr (0.06 mol/L) solvent system. The flow rate was 0.5 mL/min, detection was by UV, and calibration was based on polystyrene standards. Qualitative solubility was determined using 0.01 g of polymer in 2 mL of solvent. A Du Pont 9900 differential scanning calorimeter and a Du Pont 9900 thermogravimetric analyzer were then employed to study the transition data and thermal decomposition temperature of all the polymers. The differential scanning calorimeter (DSC) was run under a nitrogen stream at a flow rate of 30 cm^3/min and a heating rate of 20 /min. The thermogravimetric analysis (TG) was determined under a nitrogen flow of 50 cm^3/min. Dynamic mechanical analysis (DMA) was performed on a Du Pont 9900 thermal analyzer system. A sample 10 mm in length, 2 mm in width, and approximately 0.05 mm in thickness was used. The dynamic shear modulus was measured at a resonance mode and an amplitude of 0.2 mm. The

Scheme 1

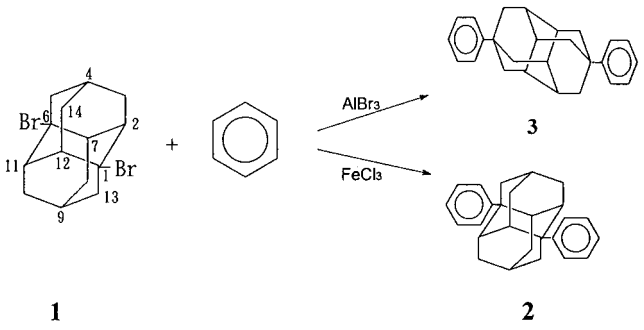

wide-angle X-ray diffraction measurements were performed on a Philips PW 1730−10 X-ray diffractometer using Cu K_α radiation.

Tensile properties were determined from stress−strain curves with a Toyo Baldwin Instron UTM-III-500 with a load cell of 10 kg at a drawing speed of 5 cm/min. Next, measurements were performed at 28 °C with film specimens (about 0.1 mm thick, 1.0 cm wide, and 5 cm long) and an average of at least five individual determinations was used. The in-plane, linear coefficient of thermal expansion (CTE) was obtained from a TA TMA-2940 thermomechanical analyzer (5 °C/min, from 50 to 250 °C, 10 mN). The CTE value on the temperature scale between 50 and 200 °C was recorded after an initial conditioning step (heat to 250 °C, hold 5 min, and cool). Moisture absorption measurements were made with an ultramicrobalance of Sartorius model S3D−P on thin film (~40 μm). Measurements were taken at 30 °C for 90 h at 85% relative humidity. The dielectric constant was measured by the parallel-plate capacitor method using a dielectric analyzer (TA Instruments DEA 2970) on thin films. Gold electrodes were vacuum deposited on both surfaces of dried films, followed by measurement at 25 °C in a sealed humidity chamber at 0% relative humidity.

Polymer Synthesis by the Two-Step Method. Dianhydride **6d** (0.444 g, 1.00 mmol) was added to a stirred solution of **5** (0.370 g, 1.00 mmol) in NMP (solid content 10% w/v) under N_2 at ambient temperature for 6 h. The inherent viscosity of the poly(amic acid) **7d** in NMP was 0.65 dL/g, measured at a concentration of 0.5 g/dL at 30 °C. The IR spectrum exhibited absorptions at 3345 (N−H and O−H str), and 1720, 1650 cm^{-1} (C=O str), i.e., characteristic of the amic acid. The poly(amic acid) solution was then cast onto a glass plate. The poly(amic acid) **7d** was converted to polyimide **8d** by successive heating in a vacuum at 80 °C for 3 h, at 200 °C for 8 h, and then at 320 °C for 6 h. The inherent viscosity of **8d** was 0.45 dL/g, measured at a concentration of 0.5 g/dL in *o*-chlorophenol at 30 °C. The number-average molecular weight (M_n) of polyimide **8d** was 15 000. The symmetric and asymmetric carbonyl stretches occur at 1780 and 1723 cm^{-1} in the FTIR spectrum of **8d**. Other associated bands are the C−N stretch at 1368 cm^{-1} and the band at 710 cm^{-1}, i.e., the deformation of the imide ring to imide carbonyls. The other polyimides were prepared in a similar manner from **5** and aromatic tetracarboxylic dianhydrides.

Results and Discussion

Monomer Synthesis. 1,6-Bis(4-aminophenyl)diamantane (**5**) was synthesized from **1** and then reacted with benzene in the presence of iron(III) chloride as a catalyst to generate **2** as shown in Scheme 1 and 2. Interestingly, using a different catalyst, i.e., aluminum bromide, **1** reacted with benzene to generate 4,9-diphenyldiamantane (**3**). Chapman et al. also reported that selective functionalization of 1-bromodiamantane to the major product 4-phenyldiamantane could be obtained with aluminum chloride used as the catalyst.[24] This finding is attributed to the fact that the kinetically favored medial products (1-phenyldiamantane) equilibrate to the apical products (4-phenyldiamantane) under thermodynamic control.[24] Next, **2** reacted with fuming nitric acid in the presence of glacial acetic acid to generate **4** in high yield. According to our results, the aromatic region of **2** provided evidence of overnitration when in the presence of a higher concentration of fuming nitric acid. In addition, **4** was hydrogenated to obtain compound **5**. On the basis of the carbon shielding effect, the positions of chemical shifts for carbons of **5** were readily assigned from a DEPT experiment in Figure 1 A. With the aid of a 2D $^1H-^{13}C$ COSY spectrum of **5**, the positions of chemical shifts for protons of **5** was readily assigned as shown in Figure 1B. An equatorial proton was found further downfield by ~0.46 ppm than the axial proton on the individual carbon atom (C-3, 8, 10, 14) in a rigid diamantyl ring. Its presence is attributed to that the equatorial proton is within the deshielding cone of the neighboring C−C bond. The signal at 3.54 ppm is peculiar to the amino group. When **4** was converted into the diamine **5**, the resonance of protons H_c was found further to high field from 8.21 to 6.67 ppm (see Experimental Section). X-ray diffraction analysis also confirmed the structure of **4**. X-ray crystal data for **4** was acquired from a single crystal, as obtained by slowly crystallizing from DMF solution of **4**. The structure of **4** exhibited molecular symmetry. Figure 2 depicts the X-ray structure of **4**. On the other hand, the elemental analysis data, the NMR spectra, and the IR spectra confirmed the presence of all new compounds.

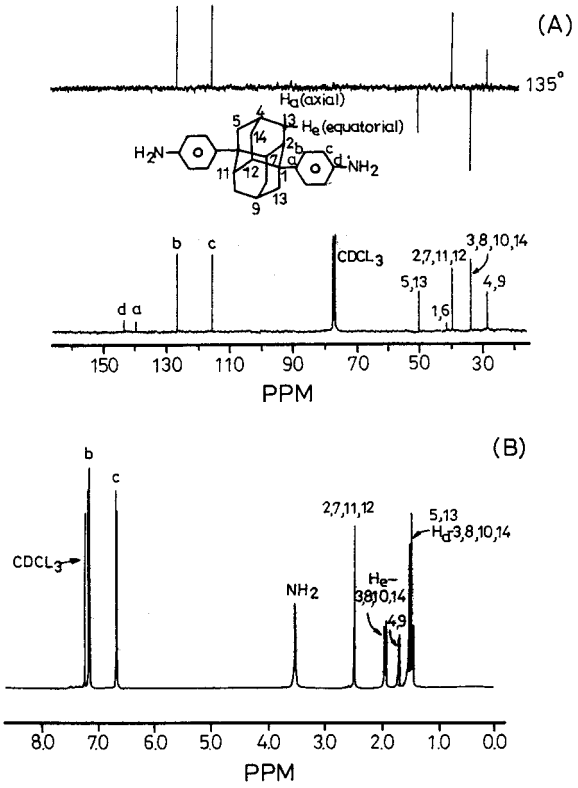

Figure 1. NMR ($CDCl_3$) spectra of 5. (A) ^{13}C 135° DEPT and ^{13}C NMR (100 MHz); (B) ^1H NMR (400 MHz).

Synthesis of Polymers. New diamantane-based polyimides were synthesized by a conventional two-step procedure starting from **5** and aromatic tetracarboxylic dianhydrides **6** through the ring-opening polyaddition and subsequent thermal cyclodehydration, as shown in Scheme 3. Table 1 summarizes those results. The ring-opening polyaddition in NMP at room temperature

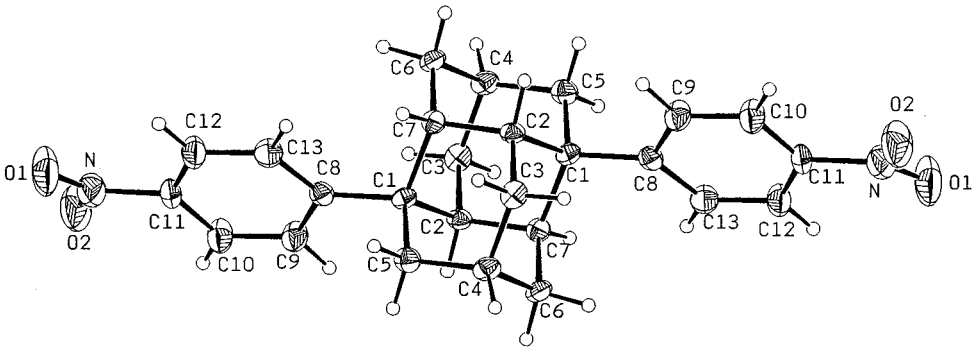

Figure 2. X-ray structure of **4**.

Scheme 2

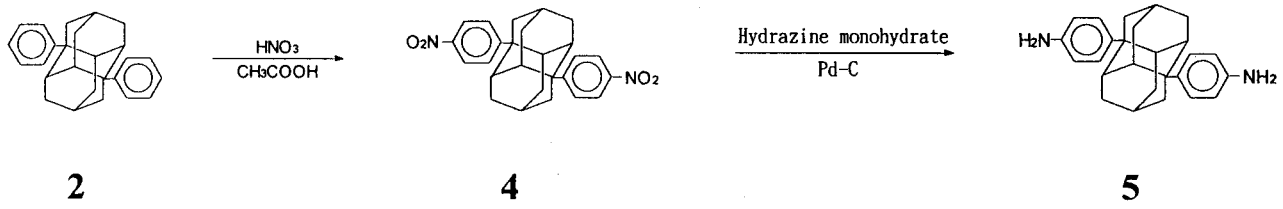

2 **4** **5**

Scheme 3

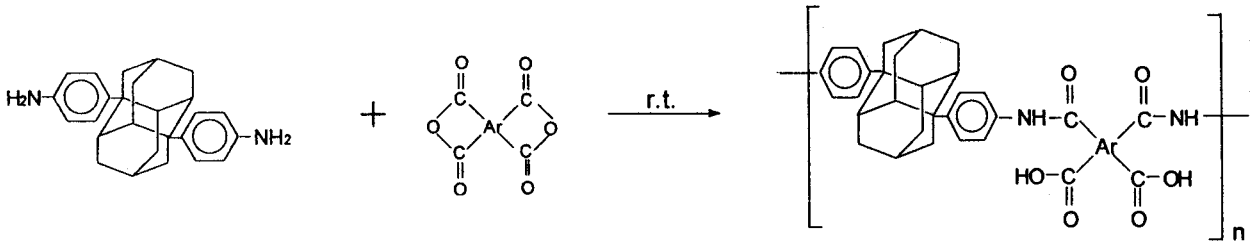

5 **6** **7**

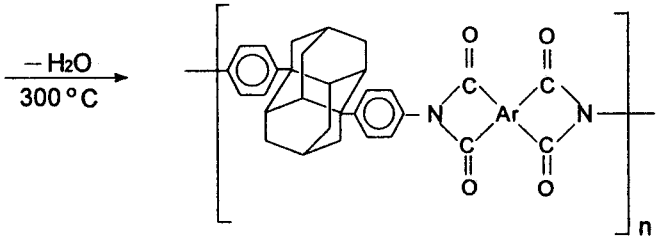

8

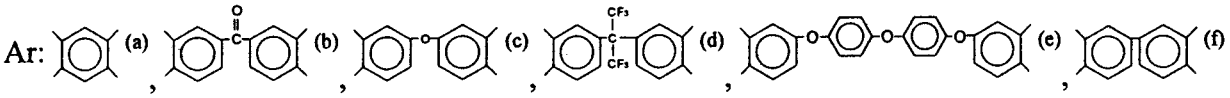

yielded poly(amic acid)s **7** with medium and high inherent viscosities between 0.65 and 1.41 dL/g. The IR spectroscopy confirmed the formation of poly(amic acid)s **7**. The characteristic absorption bands of the amic acid appeared near 3345 (N−H and O−H str), 1720 (acid, C═O str), 1650 (amide, C═O str), and 1540 cm^{-1} (N−H bending). The thermal conversion to polyimides **8** was performed by successively heating the poly(amic acid)s **7** to 320 °C in a vacuum. The soluble polyimides **8d** and **8e** had inherent viscosities of 0.45 and 0.49 dL/g, respectively. According to GPC data, M_n and M_w/M_n of polyimide **8d** were 15 000 and 1.7, respectively. The M_w/M_n valve was actually lower than those of the commerical materials, which may be due to the somewhat low reactivity of **5** containing the rigid and bulky diamantyl element. IR spectroscopy confirmed the formation of polyimides **8**. The characteristic absorption bands of the imide ring appeared near 1780 (asym C═O str), 1720 (sym C═O str), 1390 (C−N str), and 745 cm^{-1} (imide ring deformation). In addition, as Figure 3 indicates, NMR spectra confirmed the polyimide **8d**. In the proton, i and j were assigned while assuming that

Table 1. Inherent Viscosities and GPC Molecular Weights of Poly(amic acid)s and Soluble Polyimides

dian-hydride	poly(amic acid)s	polyimides		
	η_{inh}[a] (dL/g)	$M_n \times 10^{-4}$	M_w/M_n	η_{inh}[b] (dL/g)
6a	1.41	*d*		
6b	0.81			
6c	0.97			
6d	0.65	1.5[c]	1.7	0.45[b]
6e	0.77			0.49[b]
6f	0.84			

[a] Measured in NMP at 0.5 g/dL at 30 °C. [b] Measured in *o*-chlorophenol at 0.5 g/dL at 30 °C. [c] By GPC (relative to polystyrene). [d] Could not be measured.

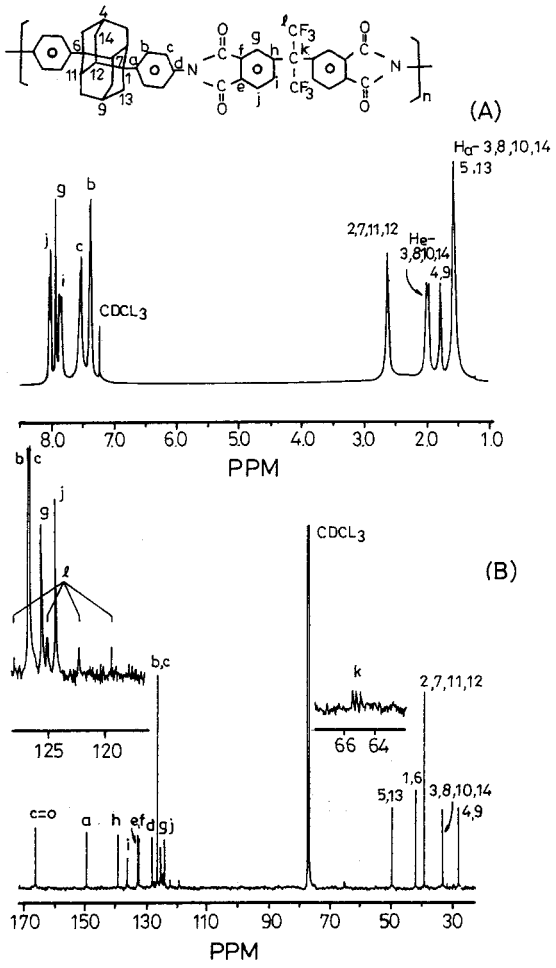

Figure 3. NMR ($CDCl_3$) spectra of polyimide **8d**. (A) ^1H NMR (400 MHz); (B) ^{13}C NMR (100 MHz).

the j proton ortho to the C═O had shifted farther downfield. Also, the i proton signal was broadened through interaction with the nearby CF_3 groups and, possibly, by unresolved meta coupling with the g proton. Herein, the ^{13}C NMR spectrum of **8d** was assigned using a combination of DEPT, 2D $^1H-^{13}C$ COSY, and the results for carbon assignments in compound **4**. In the carbon, the e and f assignments were made while assuming that the e carbon para to the $C(CF_3)_2(Ph)$ had shifted farther downfield. Splitting of the k carbon absorption was observed due to long-range effects by the CF_3 fluorine. Similarly, the l carbon absorption was split into the quartet by the fluorine.

Characterization of Polymers. The polyimides solubilities were tested in various solvents. Table 2 summarizes those results. Owing to the bulky diamantyl elements and flexible ether segments, the non-

Table 2. Solubilities of Polyimides[a]

solvent	solubility for polymer					
	8a	**8b**	**8c**	**8d**	**8e**	**8f**
o-chlorophenol	−	−	+−	+	+	+−
m-cresol	+−	+−	+−	+−	+−	+−
chloroform	−	−	+−	++	+−	−
THF	−	−	−	+	−	−
NMP	−	−	−	+−	−	−
DMAc	−	−	−	++	−	−

[a] Solubility: ++, soluble at room temperature; +, soluble on heating at 60 °C; +−, partial soluble on heating at 60 °C; −, insoluble on heating at 60 °C. Abbreviation: NMP, *N*-methyl-2-pyrrolidone; DMAc, *N*,*N*-dimethylacetamide; THF, tetrahydrofuran.

fluorinated polyimide **8e** could be soluble in *o*-chlorophenol. The hexafluoroisopropylidene-containing polyimide **8d** exhibited an excellent solubility toward test solvents. The polyimide **8d** could be soluble in *o*-chlorophenol, chloroform, DMAc, and THF. The reason for the excellent solubility of **8d** was explained as follows. The bulky CF_3 groups force noncoplanarity between the phenylene rings and the hexafluroisopropylidene groups to take up increased spatial volume which hinders packing of the polymer chain and hence increases the solubility. In addition, in the bulky and polar CF_3 groups in the polymers under consideration, perhaps these forces of attraction are significantly weakened by a combination of steric and dipolar repusive force that prevents spontaneous parallel aligment of the rodlike molecules. Thus, the solubility of **8d** was high. However, the other polyimides **8** were insoluble in the test solvents due to the presence of the relatively rigid structures in the dianhydride moieties. Transparent and pale yellowish colors of polyimide films **8** were obtained by successively heating the corresponding poly(amic acid)s **7**. The polyimide films **8** were structurally characterized initially by X-ray methods. All polyimides **8** had nearly the same amorphous patterns with broad peaks appearing (2θ) at around 18°.

Table 3 summarizes the dielectric constants, moisture absorptions, CTEs, and mechanical properties of polyimides **8**. The mechanical properties were determined via an Instron machine. All polyimides **8**, except **8a**, **8d**, and **8f**, exhibited high tensile strengths up to 124 MPa. All polyimides **8** were fractured in a brittle manner under the tensile test. Thus, the elongation to break values of polyimides **8** were low. This phenomena is attributed to that the polyimides **8** contain the extremely rigid and bulky 1,6- diphenyldiamantyl element. However, the polyimides **8a**, **8d**, and **8f** were brittle due to the relatively rigid structures in the dianhydride moieties.

The moisture absorptions of polyimides **8** are very small, i.e., less than 0.40%, because of the waterproofing effect of the diamantane elements. The polymers absorbed moisture heavily influences their dielectric constants. Table 3 also indicates that the dielectric constants of diamantane-based polyimides **8** are quite low: ranging from 2.54 to 2.74. Even the nonfluorinated polyimides **8** also have low dielectric constants. Such low dielectric constants are due to the fact that diamantane is a fully aliphatic hydrocarbon, subsequently leading to low hydrophobicity and polarity. We speculate that this event is due to the "dilution" effect of the polar imide groups by the diamantyl groups (on a weight basis based on polymer).

Table 3. Physical Properties of Polyimide Films

polymer	strength to break (MPa)	elongation to break (%)	initial modulus (GPa)	CTE[a] (ppm/°C)	% H_2O absorption[b] 85 % RH	dielectric constant[c] (dry, 1 kHz)
8a	28.7	0.56	2.1	117	0.208	2.65
8b	59.2	1.5	2.3	113	0.389	2.74
8c	124.0	5.6	2.2	105	0.236	2.66
8d	25.1	1.1	2.3	91	0.207	2.54
8e	68.0	2.9	2.2	108	0.224	2.67
8f	19.8	0.74	2.0	112	0.240	2.66

[a] The CTE value was measured on the temperature scale between 50 and 200 °C. [b] Moisture absorption of polyimide films were measured at 30 °C for 90 h. [c] Polyimide films were measured at 0% relative humidity and 25 °C.

Table 4. Thermal Properties of Polyimides

	DMA[a]			dec temp[b] (°C)	
polymer	T_g (°C)	T_β (°C)	$T_{\beta 2}$ (°C)	in air	in N_2
8a	>500	300	150	512	528
8b	>500	300	188	515	520
8c	>500	300	175	511	528
8d	>500	300	200	484	510
8e	>500	300	150	500	516
8f	*c*			526	545

[a] The glass and subglass transitions measured by DMA using shear mode at a heating rate of 5 °C/min. [b] Temperature at which 5% weight loss recorded by TG at a heating rate of 10 °C/min. [c] The film could not be measured.

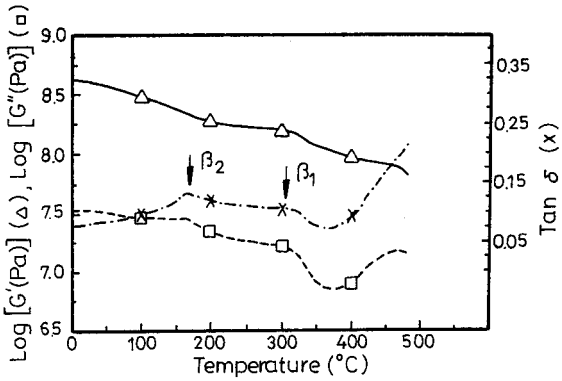

Figure 4. Dynamic mechanical analysis curves for **8c** at a heating rate of 5 °C/min.

Table 3 indicates that the CTEs of polyimides **8** resemble those of flexible polyimides.[25] In principle, all these polyimides have extremely rigid structures and would therefore be expected to have low in-plane CTE in films. However, the steric bulk of the diamantyl groups combines to disturb the orientation process which occurs during film formation, resulting in the relatively high CTE. This result is similar to the observation that the rodlike polyimides derivated from 9,9-diphenyl-2,3,6,7-xanthenetetracarboxylic dianhydride (PPXDA) with the two phenyl side groups have high CTE.[7] In addition, producing a polyimide film from polyimide solution generally leads to a lower CTE than that observed for the corresponding poly(amic acid).[7] The polyimide films **8** using for measuring CTE were obtained by casting from the corresponding poly(amic acid). Thus, the CTEs of polyimides **8** are moderate. The reason for the lower CTE from polyimide solution rather than the poly(amic acid) still remains uncertain. Auman et al. reported that the polyimide-prepared film had a much higher orientation during the film-forming process than the poly(amic acid)-prepared film.[7] In addition, I believe that the cyclodehydration process and the release of H_2O molecules during imidization process combine to disturb the molecular orientation which occurs during film formation of the poly(amic acid). In other words, we believe that the film shrinkage during imidization and the resulting possible disturbance of molecular orientation also are important in the achievement of high TCE.

Thermal analysis was performed according to DSC, DMA, and TGA. Table 4 summarizes those results. These polyimides **8** did not decompose until 400 °C in air and nitrogen atmosphere. Their temperatures at a 5% weight loss ranged from 484 to 526 °C in air and from 510 to 545 °C in N_2 atm. The influences of residual water or solvent and history of thermal annealing were occasionally observed in the initial DSC heating run. Therefore, the first heating of the samples was curtailed at 400 °C. In addition, T_g and other thermal properties were assessed according to the DSC charts of the second heating. All polyimides **8** did not show typical glass transitions. This absence is attributed to that the bulky and rigid 1,6-diphenyldiamantyl element increases the polymers **8** chains rigidity which, subsequently, produce high glass transition temperatures of **8** exceeding 500 °C.

More detailed information can be obtained from the dynamic mechanical behavior measurements taken of the films as a function of temperature. Films of about 50 μm thickness were examined on the temperature scale between 0 and 500 °C. Figure 4 illustrates the mechanical relaxation spectra of polyimide **8c**. Three relaxations were observed at ca. 175, 300, and ~500 °C, based on tan δ and G'' peaks. The low-temperature transition, termed β_2, (ca. 175 °C) is a typical relaxation for standard polyimides. This relaxation is associated with approximately a $^1/_4$ order of magnitude decrease in G'. Such a transition can generally be accounted for by the rotation or oscillations of the phenyl groups within the polyimide diamine moiety.[19,20] The second transition, termed β_1, is associated with a step decrease in G'. Small transition peaks in tan δ and G'' appear in the β_1 transition. The subglass β_1 relaxation in the polyimide **8c** is less prominent than the glass relaxation. Moreover, the β_1 relaxation of **8c** occurred at a markedly higher temperature (at 300 °C) than is typically observed in most other polyimides. The actual reason for this transition still remains uncertain. In an investigation of the polyimides based on the rigid dianhydrides and diamines, Coburn et al. also reported that high subglass relaxation at 300 °C occurred in the rigid rodlike polyimides based on a variety of 2,2′-disubstituted benzidines and rigid dianhydrides.[21] From the above results, we can infer that this high subglass relaxation at around 300 °C seems to occur in the very rigid polyimides. The temperature of this last transition from a glass state to a rubbery plateau cannot be determined precisely from the mechanical relaxation spectra of **8c**. This inability is attributed to that the T_g of **8c** exceeds 500 °C, due to incorporation of the

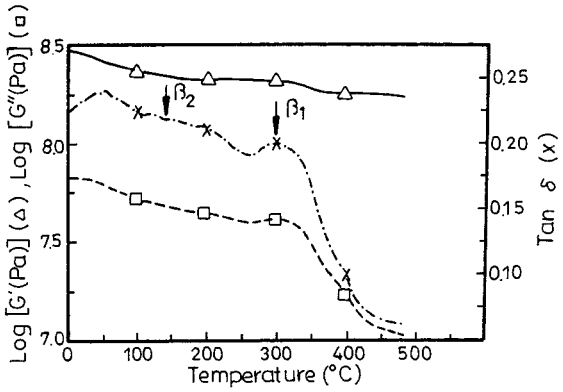

Figure 5. Dynamic mechanical analysis curves for **8a** at a heating rate of 5 °C/min.

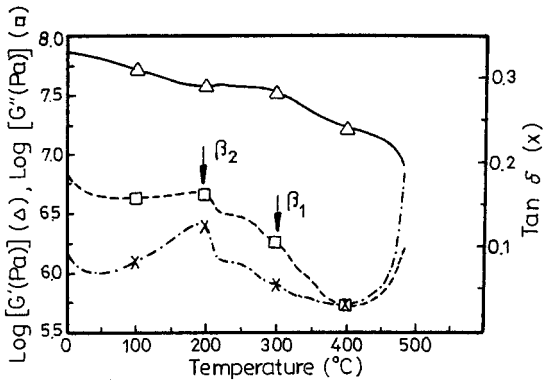

Figure 6. Dynamic mechanical analysis curves for **8b** at a heating rate of 5 °C/min.

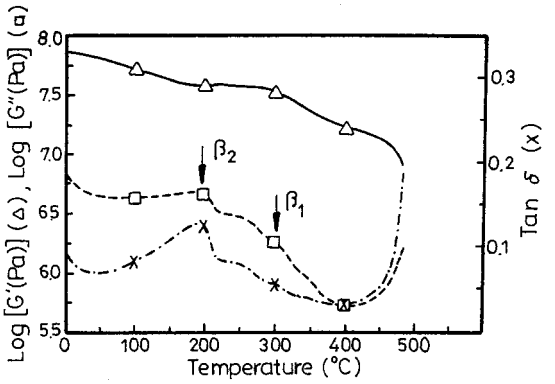

Figure 7. Dynamic mechanical analysis curves for **8d** at a heating rate of 5 °C/min.

extremely rigid and bulky 1,6-diphenyldiamantyl element in the polyimide **8c** backbone.

Figures 5−8 depict the mechanical relaxation spectra of polyimides **8a**, **8b**, **8d**, and **8e**, respectively. In all four polyimides, their relaxation spectra resemble those of **8c**. Three relaxation transitions also occurred in all four polyimides **8** on the temperature scale between 0 and 500 °C. However, the low-temperature subglass relaxation, termed β_2, did not occur at a same temperature in all four cases. The higher relaxation temperatures in β_2 arose when the polyimides **8**, except **8a**, were incorporated with the more rigid anhydride moieties (Table 4). However, the β_2 relaxation of polyimide **8a** is extremely broad in tan δ. The relatively high temperature β_1 subglass transitions at 300 °C in all four cases are also associated with a step decrease in G' and small transition peaks in tan δ and G''. The insensitivity of subglass β_1 relaxation to changes in the dianhydride confirms that the subglass process is localized largely within the diamine moiety. Thus, we believe that the motion of rigid diamantyl groups is associated with the relaxation process. In addition, the polyimides **8** possess high T_gs exceeding 500 °C. The extremely high T_g is attributed to the fact that the rotation of these bonds are hindered by the rigid and bulky 1,6-diphenyldiamantyl groups, resulting in an increasing chain stiffness.

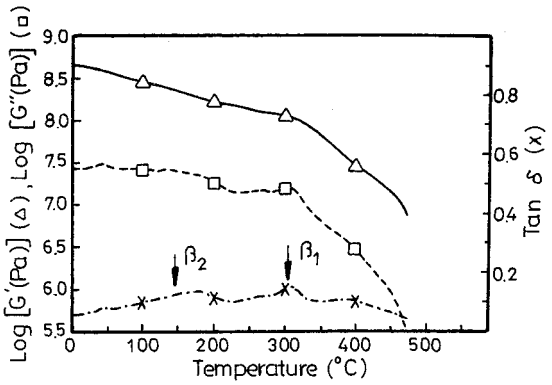

Figure 8. Dynamic mechanical analysis curves for **8e** at a heating rate of 5 °C/min.

Comparing the mechanical behaviors of the systems studied herein with those of other polyimides in a study by Coburn[21] reveals that, in both cases, extremely high temperature subglass relaxations occurred at 300 °C. Moreover, both cases have a similar insensitivity of subglass β_1 relaxation to changes in the dianhydride. Herein, small transition peaks appear in tan δ and G''. However, the polyimides derived by Coburn exhibited a rather prominent subglass relaxation. From both cases, the unusually high subglass relaxation seems to occur in the polyimides with extremely rigid backbones.

Conclusions

This work has synthesized new diamantane-based polyimides by a conventional two- step procedure starting from **5** and aromatic tetracarboxylic dianhydrides through ring-opening polyaddition, yielding poly(amic acid)s **7** with medium and high inherent viscosities between 0.65 and 1.41 dL/g, and subsequent thermal cyclodehydration. Nonfluorinated polyimide **8e** could be soluble in *o*-chlorophenol. Fluorinated polyimides **8d** was soluble in *o*-chlorophenol, chloroform, DMAc, and THF. Transparent and pale yellow polyimide films were obtained by casting from the corresponding poly(amic acid)s. All polyimides **8**, except **8a**, **8d**, and **8f**, exhibited high tensile strengths of 59.2−124.0 MPa. Their dielectric constants are notably low, ranging from 2.54 to 2.74. Three transitions occurred in all polyimides **8** and are observed by means of DMA. The low-temperature subglass relaxation, termed β_2, is a typical β relaxation for standard polyimides. Their temperatures in β_2 transitions vary widely. The relatively high-temperature β_1 relaxations occur at a much higher temperature approximately 300 than typically observed in most other polyimides. The characteristic β_1 relaxation is associated with a step decrease in G' and small transition peaks in tan and G″. Moreover, the insensitivity of the subglass β_1 relaxation temperature to changes in the dianhydride confirms that the subglass process is localized largely within the diamine moiety. Their glass relaxations occur at extremely high temperatures exceeding 500 °C. Owing to the bulky 1,6-

diphenyldiamantyl groups and loosening of the molecular packing in the films, the CTEs of these films are moderate. Interestingly, selective functionalization of 1,6-dibromodiamantane to 1,6- and 4,9-diphenyldiamantanes is achieved using the catalysts $FeCl_3$ and $AlBr_3$, respectively.

Acknowledgment. We are grateful to the National Science Council of the Republic of China for the support of this work.

References and Notes

(1) Harris, F. W.; Hsu, S. L.-C. *High Perform. Polym.* **1989**, *1*, 1.
(2) Oishi, Y.; Ishida, M.; Kakimoto, M. A.; Imai, Y. *J. Polym. Sci. Polym. Chem.* **1992**, *30*, 1027.
(3) Misra, A. C.; Tesoro, G.; Hougham, G.; Pendharkar, S. M. *Polymer* **1992**, *33*, 1078.
(4) Kim, W. G.; Hay, A. S. *Macromolecules* **1993**, *26*, 5275.
(5) Eastmond, G. C.; Paprotny, J. *Macromolecules* **1995**, *28*, 2140.
(6) Falcigno, P. A.; Jasne, S.; King, M. *J. Polym. Sci. Polym. Chem.* **1992**, *30*, 1433.
(7) Trofimenko, S.; Auman, B. C. *Macromolecules* **1994**, *27*, 1136.
(8) Feiring, A. E.; Auman, B. C.; Wonchoba, E. R. *Macromolecules* **1993**, *26*, 2779.
(9) Malik, A. A.; Archibald, T. G.; Baum, K. *Macromolecules* **1991**, *24*, 5266.
(10) Dang, T. D.; Archibald, T. G.; Malik, A. A.; Bonsu, F. O.; Baum, K.; Tan, L. S.; Arnold, F. E. *Polym. Prepr. (Am. Chem. Soc., Div. Polym. Chem.)* **1991**, *32* (3), 199.
(11) Chapman, O. L.; Ortiz, R. *Polym. Prepr. (Am. Chem. Soc., Div. Polym. Chem.)* **1995**, *36* (1), 739.
(12) Chern, Y. T.; Wang, W. L. *Macromolecules* **1995**, *28*, 5554.
(13) Chern, Y. T. *Macromolecules* **1995**, *28*, 5561.
(14) Chern, Y. T.; Fang, J. S.; Kao, S. C. *J. Polym. Sci., Polym. Chem. Ed.* **1995**, *58*, 1417.
(15) Chern, Y. T.; Wang, W. L. *J. Polym. Sci., Polym. Chem.* **1996**, *34*, 1501.
(16) Chern, Y. T.; Chung, W. H. *Makromol. Chem. Phys.* **1996**, *197*, 1171.
(17) Chern, Y. T. *J. Polym. Sci. Polym. Chem.* **1996**, *34*, 125.
(18) Ikeda, R. M. *J. Polym. Sci., Polym. Lett. Ed.* **1996**, *4*, 353.
(19) Bernier, G. A.; Kline, D. E. *J. Appl. Polym. Sci.* **1968**, *12*, 593.
(20) Perena, J. M. *Angew. Makromol. Chem.* **1982**, *106*, 61.
(21) Coburn, J. C.; Soper, P. D.; Auman, B. C. *Macromolecules* **1995**, *28*, 3253.
(22) Arnold, F. E., Jr.; Bruno, K. R.; Shen, D.; Eashoo, M.; Lee, C.; Harris, F. W.; Cheng, S. Z. D. *Polym. Eng. Sci.* **1993**, *33*, 1373.
(23) Takekoshi, T.; Kochanowski, J. E.; Manello, J. S.; Webber, M. J. *J. Polym. Sci. Polym. Chem.* **1985**, *23*, 1759.
(24) Ortiz, R. Arylation Study of Adamantane and Diamantane. Ph.D. Thesis, UCLA, 1993.
(25) Matsuura, T.; Hasuda, Y.; Nishi, S.; Yamada, N. *Macromolecules* **1991**, *24*, 5001.

MA970712I